PV BASED CONVERTER WITH INTEGRATED BATTERY CHARGER FOR DC MICRO-GRID APPLICATIONS

A Thesis

Submitted to the Faculty

of

Purdue University

by

Rima Salve

In Partial Fulfillment of the

Requirements for the Degree

of

Master of Science in Electrical & Computer Engineering

August 2014

Purdue University

Indianapolis, Indiana

To my parents, Deepak and Rekha Salve.

ACKNOWLEDGMENTS

I am deeply grateful to my advisor Dr. Euzeli Cipriano dos Santos for all his guidance, help and for all the knowledge he shared with me. Another person who made this journey easier would be, Sherrie Tucker. My heartfelt thanks to all my fellow labmates because of whom this work seemed fun and interesting.

I would like to express my gratitude to all my friends and family. Special thanks to Arti, my friend, guide and much more, without whose support and encouragement this would not have been possible. I want to thank Nikhil for his patience and moral support. Last, but not the least, my deepest appreciation goes to my father, Deepak Salve, and my mother Rekha Salve who have been of great help throughout this thesis.

TABLE OF CONTENTS

Page

Page

LIST OF TABLES

LIST OF FIGURES

Figure Page

SYMBOLS

W	watt
V	volt
A	ampere
Ω	Ohm

ABBREVIATIONS

MPPT	Maximum Power Point Tracking
PV	Photovoltaic
P&O	Perturb and Observe
IC	Incremental Conductance

ABSTRACT

Salve, Rima MSECE, Purdue University, August 2014. PV Based Converter with Integrated Battery Charger for DC Micro-grid Applications. Major Professor: Dr. Euzeli Cipriano dos Santos.

This thesis presents a converter topology for photovoltaic panels. This topology minimizes the number of switching devices used thereby reducing power losses that arise from high frequency switching operations. The control strategy is implemented using a simple microcontroller that implements the proportional plus integral control. All the control loops are closed feedback loops hence minimizing error instantaneously and adjusting efficiently to system variations. The energy management between three components, namely, the photovoltaic panel, a battery and a DC link for a microgrid is shown distributed over three modes. These modes are dependent on the irradiance from the sunlight. All three modes are simulated. The maximum power point tracking of the system plays a crutial role in this configuration as it is one of the main challenge tackled by the control system. Various methods of MPPT are discussed and the Perturb and Observe method is employed and is described in detail. Experimental results are shown for the maximum power point tracking of this system with a scaled down version of the panel's actual capability.

1. INTRODUCTION AND LITERATURE REVIEW

1.1 Introduction

The sun has been useful to mankind in more ways than one. Solar energy in it's passive form has been made use of for centuries. Later, solar energy was used to heat water for household purposes. Despite these uses, the use of solar energy that actively provides usable electricity is a relatively new idea. A few decades ago, the idea of using solar energy to power homes seemed to be a farfetched thought. But rapid progress has been made over the past few years in order to make this idea a practical and viable option [1]. Todays solar photovoltaic power electronics systems have changed the image of utilizing solar energy, being limited to the drawing board [2]. These systems can be used over a variety of applications, right from powering a mobile phone to powering your home. Another important factor that needs consideration is the cost of installation of this photovoltaic system [3]. It has reduced drastically over the years. Where a system would have cost in the range of $12 per watt of energy produced in 1988, it now costs a third of that price in 2013 [4]. Though all of the above factors that make solar energy seem like an attractive option, there are still issues concerning the efficiency of the photovoltaic panels.

1.2 The Photovoltaic cell and it's evolution

The development of photovoltaic or solar cell technology began in 1839 by a French physicist Antoine-Cesar Becquerel [5]. Becquerel observed the photovoltaic effect while experimenting with a solid electrode in an electrolyte solution when he saw a voltage develop when light fell upon the electrode. The first genuine photovoltaic cell was built around 1883 by Charles Fritts, who used junctions formed by coating

selenium with an extremely thin layer of gold. This was followed by the first silicon photovoltaic cell developed by Russell Ohl in 1941, with only a fraction of improvement in efficiency than selenium cells. The beginning of the modern photovoltaic cell was in 1954 when Bell Laboratories used diffused silicon p-n junction. The electrons and holes are generated through light at the interface of pn junctions, separated by the electrical field across the pn junction, and collected through external circuits. In principle, the single crystalline silicon semiconductor can reach 92% of [6] the theoretical attainable energy conversion, with 20% conversion efficiency in commercial designs [7] [8]. However, because of the considerably high material costs, thin-film solar cells have been developed to address the product costs. Amorphous silicon is a candidate for thin-film solar cells because its defect energy level can be controlled by hydrogenation and the band gap can be reduced so that the light-absorption efficiency is much higher than crystalline silicon. The problem is that amorphous silicon tends to be unstable and can lose up to 50% of its efficiency within the first hundred hours. So, the photovoltaic cell is an all-electrical device, which produces electrical power when exposed to sunlight and connected to a suitable load. Due to the absence of moving parts inside the PV module, the wear-and-tear is very low. This significantly improves the lifetime of the module. Nonetheless, the power generation capability may be reduced to 75%-80% of nominal value due to ageing [9]. Today, commercial roof products are available that operate at approximately 15% efficiency. Bridging the gap between single-crystalline silicon and amorphous silicon is the polycrystalline-silicon film, for which a conversion efficiency of around 18% is obtained. Compound semiconductors, such as gallium arsenide (GaAs), cadmium telluride (CdTe), and copper indium gallium selenide (CIGS), receive much attention because they present direct energy gaps, can be doped to either p-type or n-type, have band gaps matching the solar spectrum, and have high optical absorbance. These devices have demonstrated single-junction conversion efficiencies of 16%32%. Although those photovoltaic devices built on silicon or compound semiconductors have been

achieving high efficiency for practical use, they still require major breakthroughs to meet the long-term goal of very-low cost [10] [11] [12].

A typical PV module is made up of around 36 or 72 cells connected in series, encapsulated in a structure made of aluminium and tedlar. A PV array is formed by connecting multiple cells in series. This configuration benefits from a high voltage of about 25V to 45V across the terminals. But the weakest cell determines the current seen at the terminals. This results in a reduction in the available power. As opposed to the series connection, the parallel connection solves the problem of the weakest link, but the voltage seen at the output is rather low.

1.3 Power Distribution Systems

1.3.1 Radial System

A traditional power distribution system is characterized by radial topology [13]. In this system, separate feeders radiate from a single substation and feed the distributors at one end only. The figure shows a single line diagram of a radial system for d.c. and a.c. distribution respectively [14]. The radial system is employed only when power is generated at low voltage and the substation is located at the center of the load [15]. This is the simplest distribution topology having a low initial cost but suffers from the following drawbacks [16]. The end of the distributor nearest to the feeding point will be heavily loaded. The consumers are dependent on a single feeder and single distributor, hence any fault in the feeder or distributor cuts off supply to the consumers who are on the side of the fault away from the substation. Another drawback is that the consumers at the distant end of the distributor would be subjected to a serious voltage fluctuation when the load on the distributor changes. As a result, this system is used to short distances only.

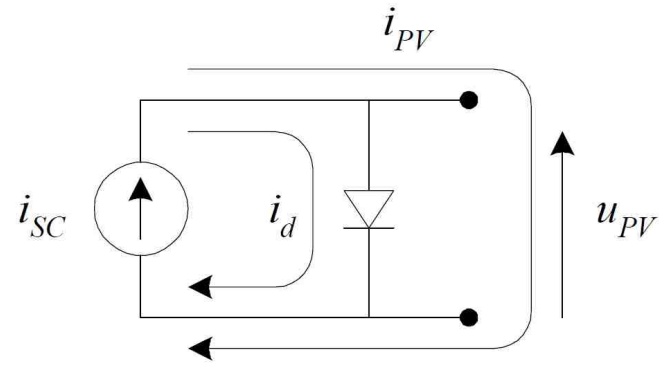

(a) Electrical model with current and voltage defined

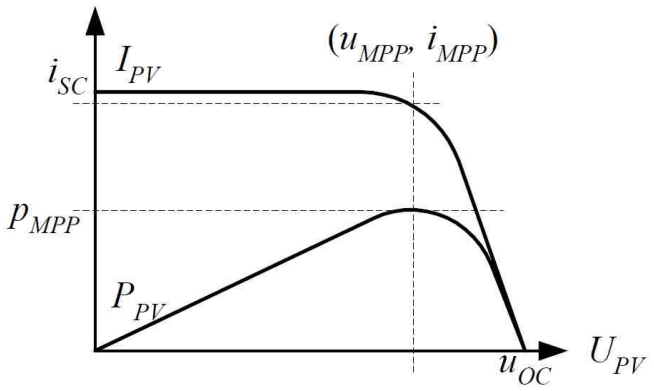

(b) Electrical characteristics of PV cell when exposed to a given amount of sunight

Fig. 1.1. Electrical model and characteristics of a photovoltaic (PV) cell

1.3.2 Ring Main System

Here, the primaries of distribution transformers form a loop. The figure shows the single line diagram of ring main system for a.c. distribution [15]. This system has certain advantages like lesser voltage fluctuations at consumers terminals. This system is also very reliable as each distributor is fed via two feeders. In the event that a fault occurs on any section of the feeder, the continuity of supply is maintained.

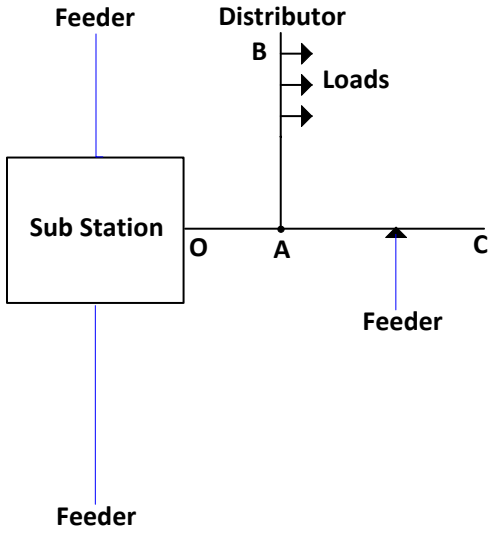

(a) d.c distribution

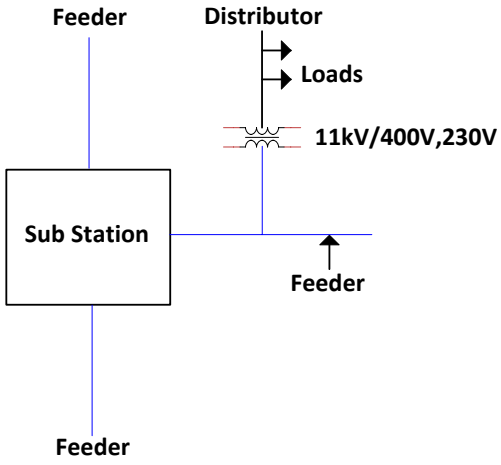

(b) a.c distribution

Fig. 1.2. Single line diagram of a radial system

1.3.3 Interconnected System

In the case where the feeder ring is energised by two or more generating stations or substations, it is called an inter-connected system [15]. The advantages of this

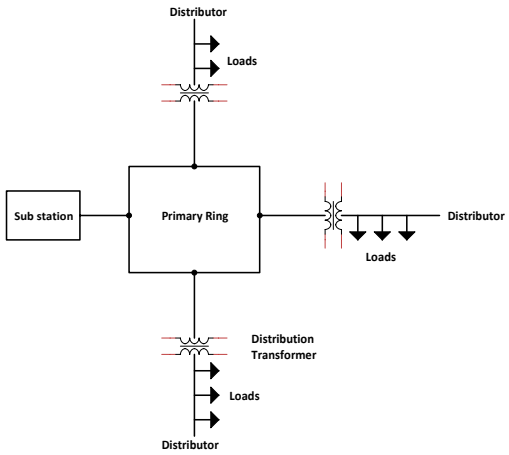

Fig. 1.3. Single line diagram of a ring main system

system is that it increases the service reliability. It reduces reserve power capacity and increases efficiency of the system as any area fed from one generating station during peak load hours can be fed from the other generating station [17].

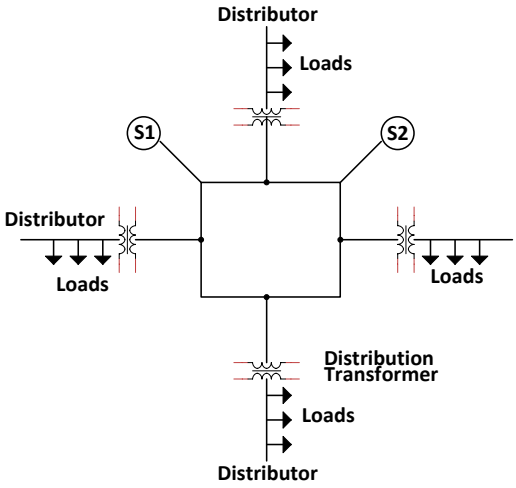

Fig. 1.4. Single line diagram of an interconnected system

Unidirectional power flow systems to supply end loads have now been replaced by new and complex systems with multiple distributed sources, active functions and bidirectional power flow capability [18] [19].

1.4 Power Converters in Power Distribution Systems

The contribution of power converters in power distribution systems is still arguable where improving system controllability, reliability, size and efficiency is concerned. Only a small part of the sunlight that reaches the PV system is converted isot useful electricity due to the inefficiency and failure-prone components used in most PV systems today [20]. High cost and lower reliability of the power converters become barriers if power electronics is used as direct, one to one, replacement for the existing electromechanical equipment. However, if the whole power distribution system were designed as a system of controllable converters, the overall system cost and reliability could actually improve [18]. In the past, power electronics converters have been mostly employed for local power conversion from an infinite source to meet dynamic energy demands of a specific load. Today, high reliability applications such as hospitals, datacom centers, and semiconductor industry, has spawned the development of super-reliable local power distribution systems with the extended use of power electronics converters. These systems include multiple primary and secondary energy sources, several levels of energy storage and back-up, and numerous active loads, all interfaced through electronic power converters [21]. All of the emerging alternative and renewable energy sources are interfaced to the existing power systems through power electronics converters due to their very different dynamic characteristics. Policy and regulatory initiatives [22] have guaranteed the use of renewable energy systems from consumer premises to centralized plants, advancing global energy sustainability and independence. Distributed power generation systems based on renewable energy sources have been considered by the exponential growth of both wind turbines and photovoltaic generation systems.

1.5 Role of Power Electronics in Renewable Energy Systems

About 40 % of the world's power needs are currently met by electrical energy and that proportion is expected to rise as countries cut carbon emissions and shift to renewable energy sources [23]. All the systems and products involved in converting and controlling the flow of electrical energy comes under the umbrella of power electronics [24]. In the case of renewable energy systems, a set of various power electronics components are required in order to convert the energy from one stage into another stage to the grid. This has to be done with the highest possible efficiency while maintaining the lowest cost possible and to keep a superior performance. As

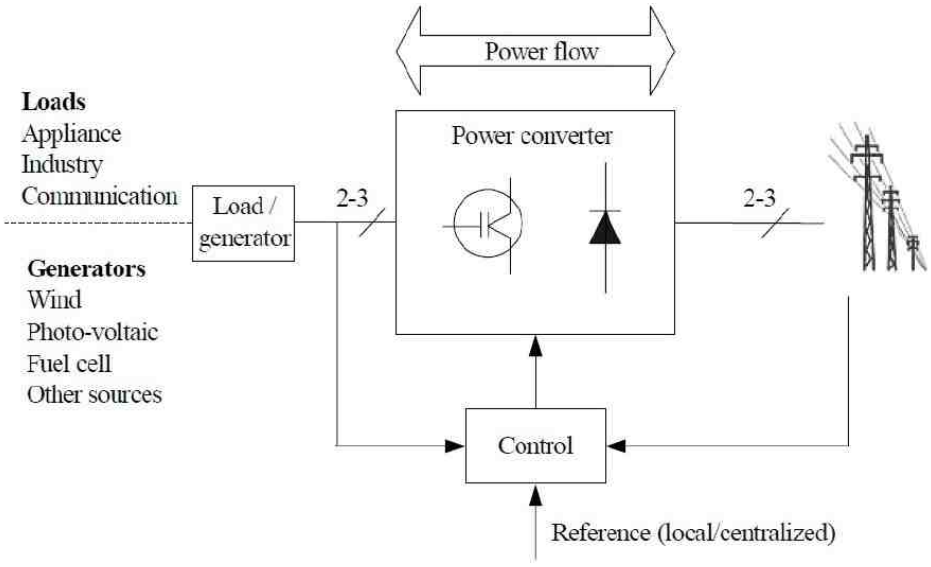

Fig. 1.5. Power electronics system with the grid, load/source, power converter and control

discussed in [9], there are three types of single-phase PV inverters. A general block diagram is shown below. It consists of PV array, PV inverter, controller and grid. PV inverters can be central inverters, string inverters or module integrated inverter [25].

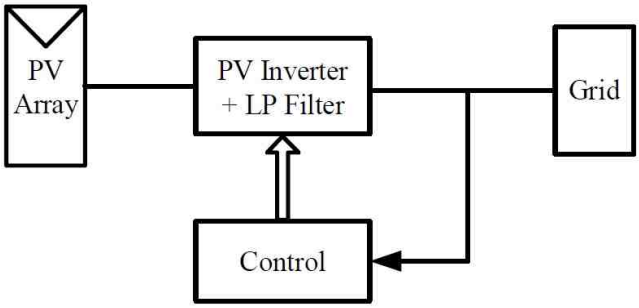

Fig. 1.6. General schematic for single-phase grid connected photovoltaic systems

1.5.1 Central Inverters

On the DC side, the single central inverter is connected to the PV plant (greater than 10kW) arranged in many parallel strings. These inverters produce high efficiency and low specific cost. Nonetheless, module mismatching and partial shading conditions give rise to decreased energy yield. The biggest drawback is that the failure of the central inverter results in the whole PV plant being out of operation.

1.5.2 String Inverters

The arrangement of the PV plant is similar to that of the central inverter. Here, each of the PV strings is assigned to a designated inverter, the so-called string inverter. This is highly beneficial when it comes to the maximum power point tracking of each PV string. This increases the energy yield.

1.5.3 Modulated Integrated Inverters

This system makes use of one inverter for each module. This topology optimizes the adaptability of the inverter to the PV characteristics as each module has its own maximum power point tracker. Although this inverter optimizes the energy yield, it has a lower efficiency than the string inverter.

1.6 Photovoltaic System Configurations

In order to generate large amounts of electricity, the PV modules are connected together to form arrays. This array is further connected with system components such as inverters to convert the DC power produced in to AC electricity for use of the consumer. This PV inverter for PV systems performs many functions.

- Converts generated DC power into AC power compatible with the utility
- Contains the protective fuctions that monitor grid connections and the PV source as well as is capable of isolating the PV array if grid problems occur
- Monitors the terminal conditions of the PV module(s) and contains the maximum power point tracking for maximizing the energy capture

1.7 Literature Review for Single Input Double Output DC-DC Converter

Many applications demand a converter with a bidirectional power flow capability to handle energy flowing from or to the source. The main focus of this thesis a converter with a configuration that allows this bidirectional power flow capability. The major applications of a dc-dc converter is in battery charging/discharging devices, uninterruptible power supplies, hybrid electric vehicle and renewable energy [26] [27].

1.7.1 Bidirectional multi-level dc-dc converter

In [28], the authors propose a bidirectional multi-level dc-dc power conversion system with multiple dc sources. In this, the output level can be changed almost continuously without any magnetic components. One of the major benefits of this magnetic-less system is that very high temperature operation is possible in comparison to conventional solutions.

1.7.2 High Power Current Sensorless Bidirectional 16-Phase Interleaved DC-DC Converter for Hybrid Vehicle Application

In [29], the authors have proposed a new 16 phase interleaved bidirectional dc/dc converter is developed featuring smaller input/output filters, faster dynamic response and lower device stresses than conventional designs, for hybrid vehicle applications. Here the converter is connected bwtween the ultracapacitor pack and the battery pack in a multisource energy storage system of a hybrid vehicle. In the case of multiphase interleaved converters a current control loop in each phase is required to avoid imbalanced current between phases. This gives rise to increased system cost and control complexity. This paper proposes operation of the converter in discontinuous conduction mode (DCM) to minimize imbalancce current and remove current control loop in each phase.

1.7.3 Bidirectional DC-DC buck converters with single-input double-output

This section will make a comparison between a direct and a proposed solution in [30]. A conventional single-input single-output dc-dc buck converter comprises of switch and diode power devices as well as inductive and capacitive elements. The direct solution for a single-input double-output converter is replicating the conventional arrangement. This implies doubling the number of components with respect to the single-input single-output converter.

From figure 1.8 it is clear that the direct solution comprises of four switches, and two inductors.

[31] proposes a single-inductor dual output switching converter topology that is able to independently regulate two output voltages. Besides making use of only one inductor, the solution uses four power switches. This is beneficial due to the reduction of one inductor.

A further improvement is made in [32] where a three switch dc-dc converter with two outputs is presented.

The topology that is proposed in [30] is shown in figure 1.9 for both bidirectional and unidirectional application of single-input double-output dc-dc buck converter. It can be observed from this that in these circuits, a power switch and diode is eliminated when compared to the direct solution as shown in Figure 1.8.

1.8 Proposed Bidirectional Converter

This configuration proposes a bidirectional single-input double-output dc-dc converter which uses three power switches along with two low pass filters. This converter has eight possible switching states as a combination of the three switches. A detailed explanation of this topology will be given in Chapter 3.

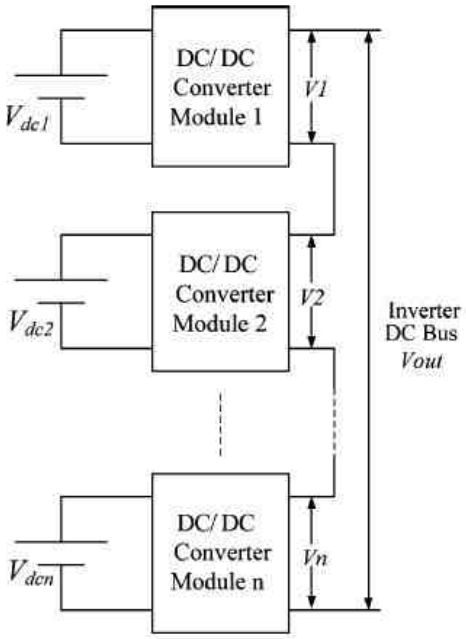

(a) DC-DC power converter system configuration

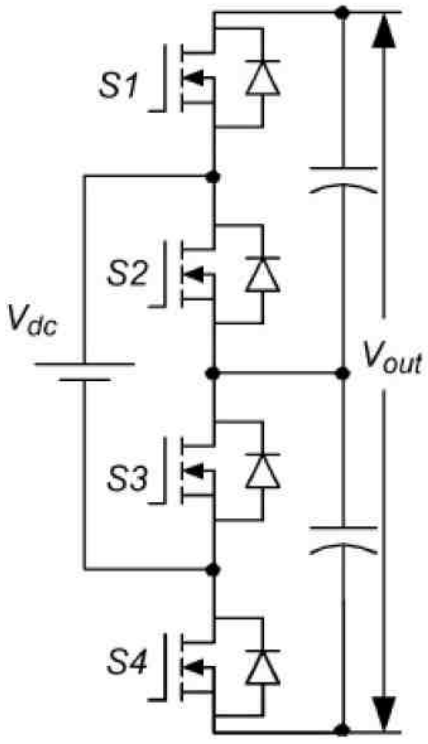

(b) topology of the dc-dc converter module

Fig. 1.7. DC-DC power conversion system configuration and converter cell topology

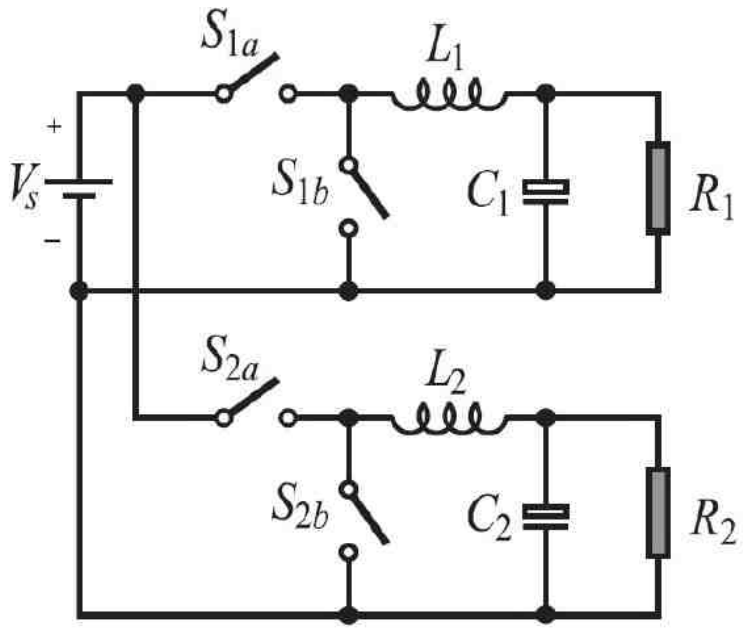

(a) Bidirectional DC-DC buck converter with single-input double-output

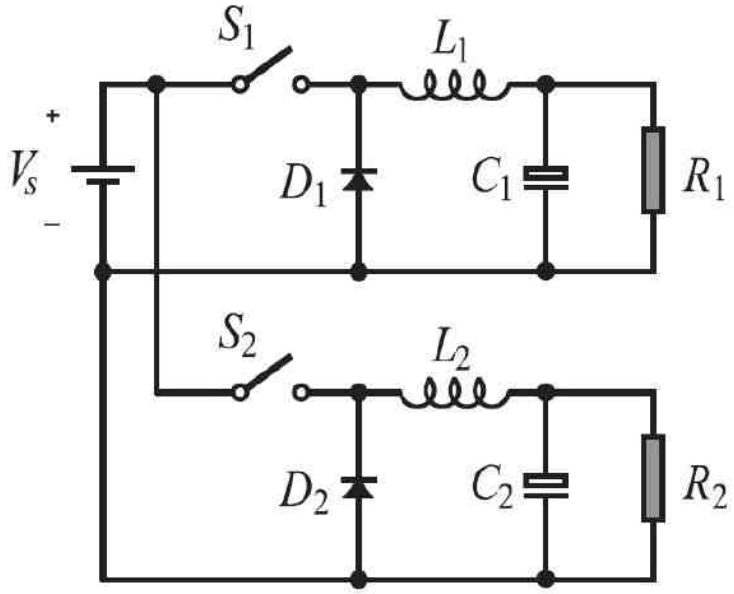

(b) Unidirectional DC-DC buck converter with single-input double-output

Fig. 1.8. Direct solution for bidirectional and unidirectional dc-dc buck converter with single-input double-out

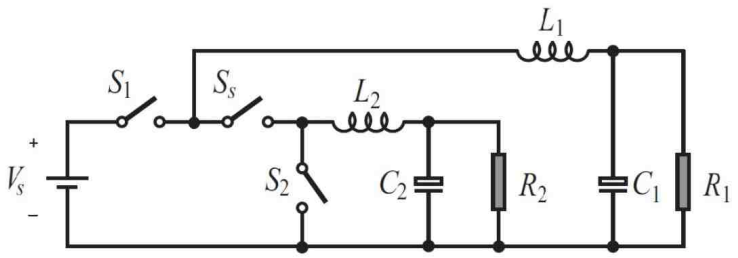

(a) Bidirectional DC-DC buck converter with single-input double-output

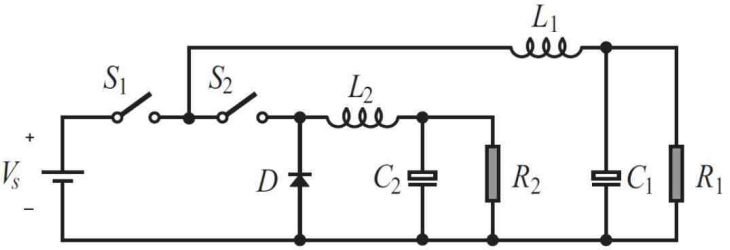

(b) Unidirectional DC-DC buck converter with single-input double-output

Fig. 1.9. Proposed solution for bidirectional and unidirectional dc-dc buck converter with single-input double-out

2. CONTROL STRATEGIES

2.1 Introduction

This chapter will discuss the role of control engineering and its importance in a system. Further it will give an overview of the different types of control systems/schemes and controllers that are commonly used today. A detailed description of the various methods employed for the control of the PV panel will be given.

2.2 Control Engineering

Control engineering or control systems engineering is the engineering discipline that applies control theory to design systems with desired behaviour [33]. The goal of control engineering is to improve, or in some cases enable, the performance of a system by the addition of sensors, control processors, and actuators. The sensors measure or sense various signals in the system and the operator commands; the control processors process the sensed signals and drive the actuators, which affect the behaviour of the system [34]. Figure 2.1 represents a variety of control systems right from an aircraft to an industrial process to a large electric power generation and distribution system. The signals can be transmitted digitally or via analog electrical signals. They can also be in the form of mechanical linkages or pneumatic lines. A control system can be of different types. Feedback, feed forward, cascade, open loop control system to name a few.

2.3 Types of Controllers and Implementation

There are different types of controllers that can be used depending on the application [35]. They can vary widely in effectiveness and complexity. Controllers can

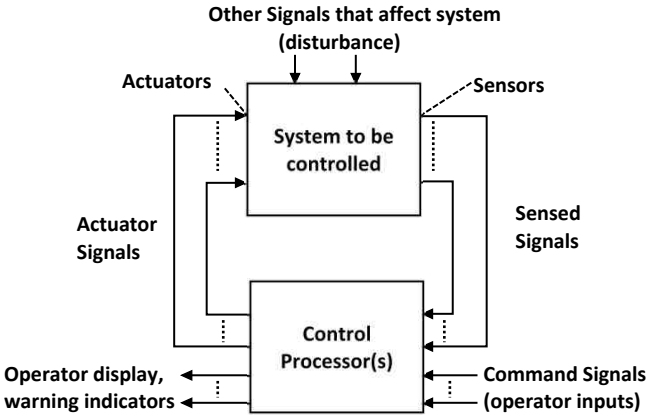

Fig. 2.1. Control System Schematic

be linear or non-linear depending on the type of system they are used to control. Linear systems are a mathematical model of a system based on the use of a linear operator [36]. They have one equilibrium point at the origin. Non-linear systems are those that do not follow the principle of superposition, have multiple isolated equilibrium points and may exhibit properties such as limit cycle, bifurcation and chaos [37]. The control processor is responsible for the implementation of the signal processing algorithm specified by the controller. Commercially available control processors can be used but are generally restricted to logic control and specific types of control laws. To implement a wide variety of control laws, general purpose digital signal processing (DSP) chips are made use of. These chips can implement complex control laws.

2.3.1 Linear Controllers

Linear controllers comprise of the proportional (P), proportional plus integral (PI), proportional plus derivative (PD) and proportional plus integral plus derivative (PID). These are the simpler of the linear controllers and find their applications in many industries [38]. More sophisticated controllers include the linear quadratic regu-

lator (LQR), the linear quadratic Gaussian (LQG), and the estimated-state-feedback controller. This thesis implements the simple linear controllers.

2.3.2 Non Linear Controllers

Many well-developed techniques for analysing nonlinear feedback systems are available [39]. A few being describing function method, phase plane method, lyapunov stability analysis and many more [40]. These methods will not be discussed as the focus of this thesis is on the application of linear controllers.

2.4 Maximum Power Point Tracking Methods

As discussed in Chapter 1, various methods are employed for maximum power point tracking (MPPT). [41] [42]. These methods range from simply controlling one parameter, to more complex methods where several parameters are controlled [43] [44]. Every method has certain advantages as well as disadvantages. The most suitable method for a specific application can be chosen depending on which parameter of the system can be compromised and which parameter is critical.

2.4.1 Constant Voltage Method

This is the simplest algorithm among the MPPT control methods [45]. The operating point of the PV array is, each nth step, kept near the maximum power point or MPP by regulating the array voltage and matching it to a fixed reference voltage V_{REF} equal to the V_{MMP} of the characteristic PV module or another pre-valuated best voltage value [46]. This method does not provide very accurate tracking.

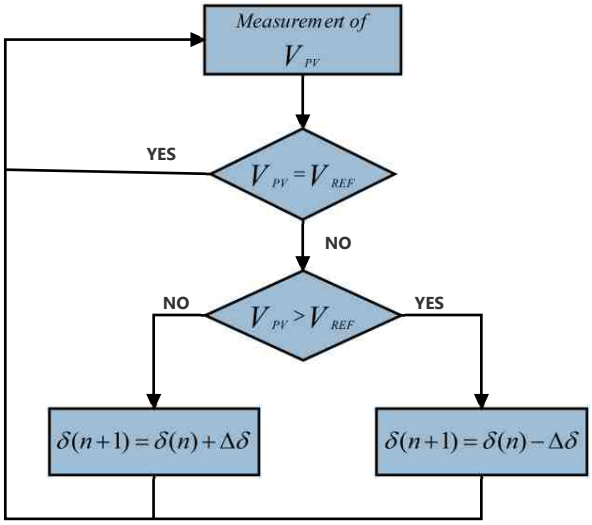

Fig. 2.2. Constant Voltage Method

2.4.2 Short-Current Pulse Method

This method achieves the maximum power point by giving a reference current I_{REF} to the power converter controller [47]. In fact, the optimum operating current for maximum output power is proportional to the short-circuit current I_{SC} under various conditions of irradiance level S as follows [48].

$I_{REF}(S) = k1.I_{SC}(S)$; where k1 is a proportional constant

2.4.3 Open Voltage Method

The Open Voltage (OV) method is based on the observation that the voltage V_{MPP} is always close to a fixed percentage of the open-circuit voltage V_{OV}. This technique uses 76 % of V_{OV} as reference value V_{REF} (obtain maximum output power).

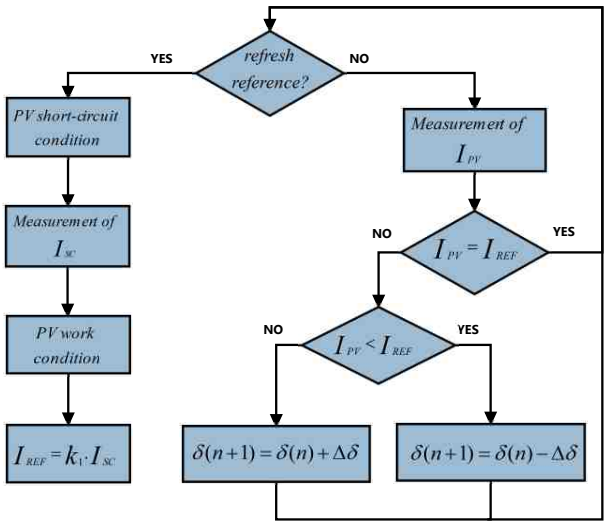

Fig. 2.3. Short-Current Pulse Method

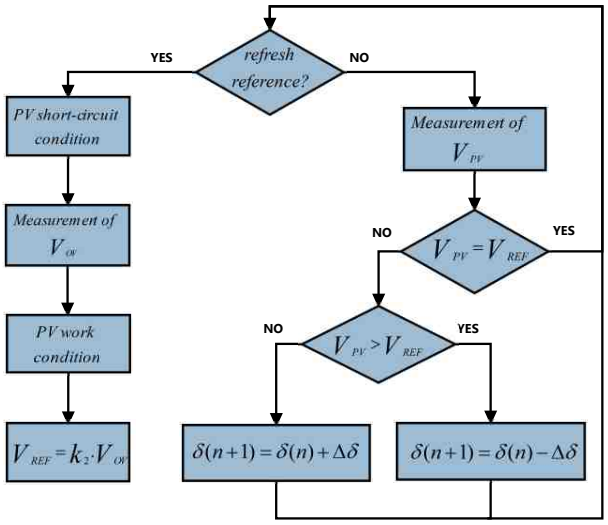

Fig. 2.4. Open Voltage Method

2.4.4 Incremental Conductance Method

The Incremental Conductance (IC) algorithm is based on the observation that the following equation holds at the maximum power point [49] [50]: $(dI_{PV}/dV_{PV})+(I_{PV}/V_{PV})=0$;

where I_{PV} and V_{PV} are the PV array current and voltage, respectively. When operating point in the P-V plane is to the right of the maximum power point, it is verified $(dI_{PV}/dV_{PV})+(I_{PV}/V_{PV}) < 0$, whereas when it is to the left of the maximum power point it is $(dI_{PV}/dV_{PV})+(I_{PV}/V_{PV}) \geq 0$. The maximum power point can thus be tracked by comparing the instantaneous conductance I_{PV}/V_{PV} to the incremental conductance (dI_{PV}/dV_{PV}). The Incremental Conductance method offers good performance under rapidly changing atmospheric conditions.

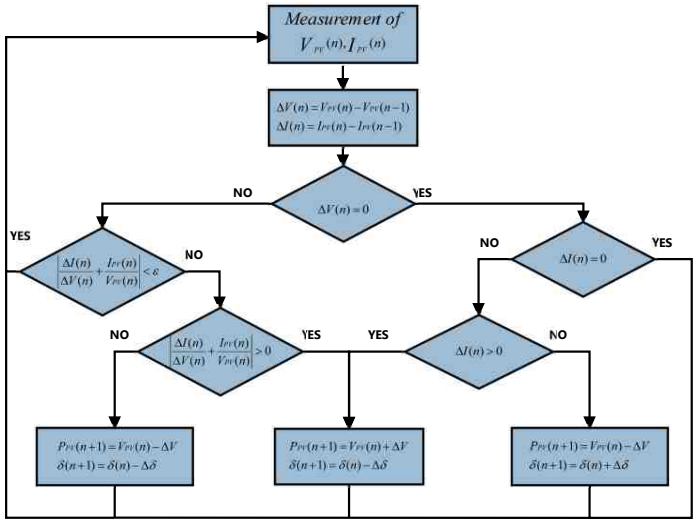

Fig. 2.5. Incremental Conductance Method

2.4.5 Perturb and Observe Method

The Perturb and Observe (P&O) method is the method used in this proposal [51] [52] [53]. This method is used as it is the optimum method which is widely used for maximum power point tracking. The method gets its name from how its working principle. This algorithm perturbs the voltage of the PV panel and measures or observes the corresponding power changes. The pertubance in voltage is done by varying the duty cycle. The aim is to follow the power v/s voltage curve and maintain

the power at its peak for a given amount of sunlight on the PV panel. If the power increases, the voltage will be continued to change in the same direction. This goes on till the power starts to decrease. This indicates that the peak power point has passed and hence the curve has to be tracked in the opposite direction in order to achieve the maximum power point once again. Figure 2.6 gives a step by step algorithm.

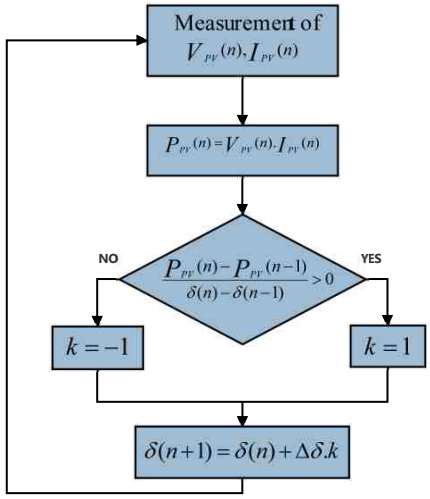

Fig. 2.6. Perturb and Observe Method

1. Measure voltage from the PV panel.
2. Measure current from the PV panel.
3. Find the power by calculating the product of voltage and current.
4. Store this power and compare it with the previous power calculated.
5. If the derivative of this difference is greater than zero, the voltage has to be increased.
6. If the derivative of this difference is less than zero, the voltage has to be decreased.
7. Repeat steps 1 through 6.

2.5 Inconsistencies In Analysis of Widely Used Control Methods

The Incremental Conductance (IncCond) method is one of the most commonly used methods for maximum power point tracking. Another method that is widely used is the Perturb & Observe method, commonly known as the P&O method. It is interesting to note a few inconsistencies between these two methods. As mentioned in [54], many papers claim that the P&O method oscillates as steady state. This issue was said to be resolved in [55] and [56] wherein it is showed that it can be made to converge at steady state. This issue is not a problem with the standard IncCond algorithm. Another consistency that is brought to our notice in [54] is in regard to the needed sensors. [57] states that 4 sensors are needed for the IncCond method, which is more than that neede for P&O method. This is contradicted in [58] where it is stated that the same number of variables are measured in both the methods. Despite all these inconsistencies, it is true that the IncCond method is slightly more complex than the PO method. This is one of the main reasons for choosing P&O method for the MPPT in this thesis. A detailed description of the P&O method is given in Chapter 3.

3. POWER ELECTRONICS CONVERTER

3.1 Introduction

This chapter provides a detailed explaination of the power electronics converter used. As mentioned in Chapter 1, this converter is a single-input double-output converter. It has three power switches and two low pass filters. This reduction in power devices used, makes a significant impact on the power loss associated with the switches. The pulse width modulation strategy for each mode is explained for the control of the duty cycle that resutls in the switching of the power switches. Further, the modification made to this configuration is explained which is the focus of this thesis. This configuration works in different modes, the details of which are explained in detail.

3.2 Bidirectional dc-dc converter

The converter proposed in [30] is a single-input double-output converter. Figure 3.1 shows the circuit diagram of this congifuration.

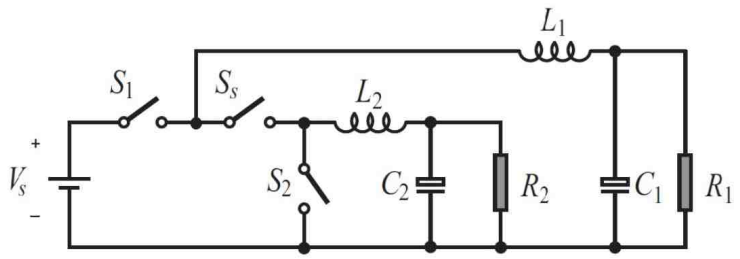

Fig. 3.1. Proposed bidirectional DC-DC converter

There are three switches S_1, S_2, and S_s. A binary variable is associated with each switch. This gives a total of eight switching states arising from the combination of these three switches. Many of these states are forbidden. A prohibited state is one which creates a situation of either a short circuit or one in which the switches would have to absorb (or dissipate) the inductive energy instantly. Hence these states are to be avoided. The switching states are given in 3.1.

Table 3.1
Topological states obtained with the states of the power switches

States	**q1**	**q2**	**qS**	**TS**
1	0	0	0	-
2	0	0	1	-
3	0	1	0	-
4	0	1	1	TS-3
5	1	0	0	-
6	1	0	1	TS-1
7	1	1	0	TS-2
8	1	0	1	-

During TS - 1 [see Fig 3.2], the input provides energy to both the loads as well as to the inductors L_1 and L_2. In this case both the inductors will be charged.

During TS -2 [see Fig 3.3], the input provides energy to load 1 and current i_{L2} flows through S_2, transferring some of its stored energy to the load 2. In this case, L_1 will be charged and L_2 will be discharged.

During TS -3 [see Fig 3.4], the current i_{L1} flows through S_s and S_2, while i_{L2} flows through S_2 transferring part of its stored energy to loads 1 and 2, respectively. In this case both the inductors L_1 and L_2 will be discharged.

Notice from Fig 3.3 that the time related to energy transfer from source to load 1 is always higher than the time related to energy transfer fro source to load 2. This

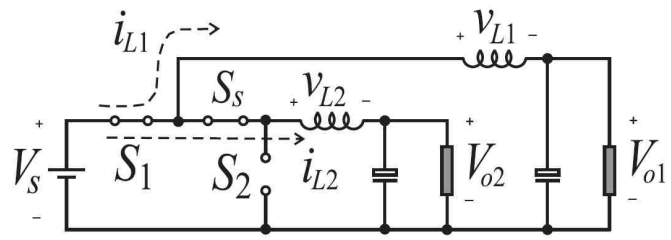

Fig. 3.2. TS - 1

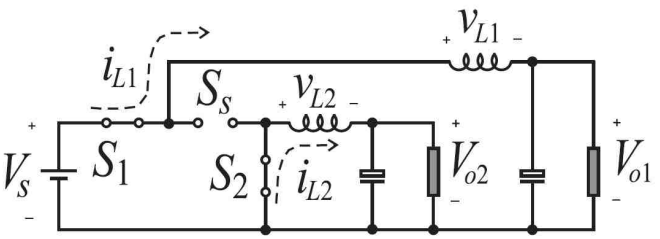

Fig. 3.3. TS - 2

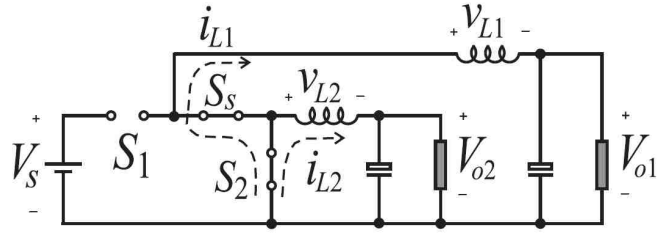

Fig. 3.4. TS - 3

being said, it is not possible to charge L_2 without charing L_1. This gives rise to a significant implication i.e. output voltage $V_{o1} \geq V_{o2}$.

3.3 Proposed modification for use of Photovoltaic panel in the configuration

A crutial modification proposed in this configuration is the replacement of the voltage source V_s with a photovoltaic panel. This modification gives rise to a number of aspects that need to be monitored and controlled. This thesis will focus on these control and power aspects that arise due to the inclusion of the photovoltaic panel. The Figure 3.5 shows the modification to the proposed solution given in [30]. Here the

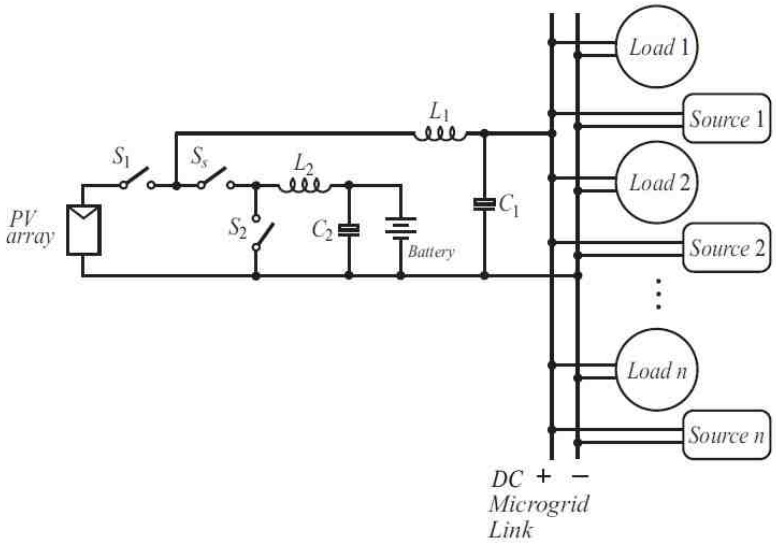

Fig. 3.5. Proposed modification to the solution given in [30]

input energy is provided by the photovoltaic panel instead of a constant DC voltage source. The primary aim of this modification is to maximize the energy from the photovoltaic panel [59] [60] [61] and minimize the energy drawn from the grid. In this case, a rechargable battery is load 1 and the DC link is load 2. The control scheme makes sure that the battery voltage is maintained along with a constant DC link voltage. Since the source of energy is not constant, several modes can be made in terms of the control aspect in order to achieve the two goals mentioned above.

The different modes are as follows:

1. Mode 1
    - PV supplies energy to the battery and the DC link.
2. Mode 2
    - Battery supplies energy to the DC link. PV non-functional.
3. Mode 3
    - Grid contributes to energy transferred to the DC link and charging of the battery. PV non-functional.

3.3.1 Mode 1 - PV to battery and DC link

This mode is as shown in Figure 3.5. Here the converter operates as a buck converter. This mode operates when the PV is exposed to sunlight and becomes the source of energy for the charging of the battery as well as supplying energy to the DC link. This mode will usually be during the day time when maximum sunlight is available. The aim of the power electronics converter in this mode is to act as a buck converter that transfers energy from the PV to the battery and DC link.

Pulse Width Modulation

The states of the three switches S_1, S_2 and S_s are controlled with the help of a proportional plus integral controller. The pulse width modulation strategy is such that it prohibits the situation of the forbidden states as listed in Table3.1. The switching frequency is set at 20kHz. The gating signals for switches S_1 and S_2 is directly controlled by the controller. The state of the switch S_s is dependent on the state of the switches S_1 and S_2. This is done to avoid the situation of the forbidden states. A OR gate is used to generate the gating signal for switch S_s. The inputs

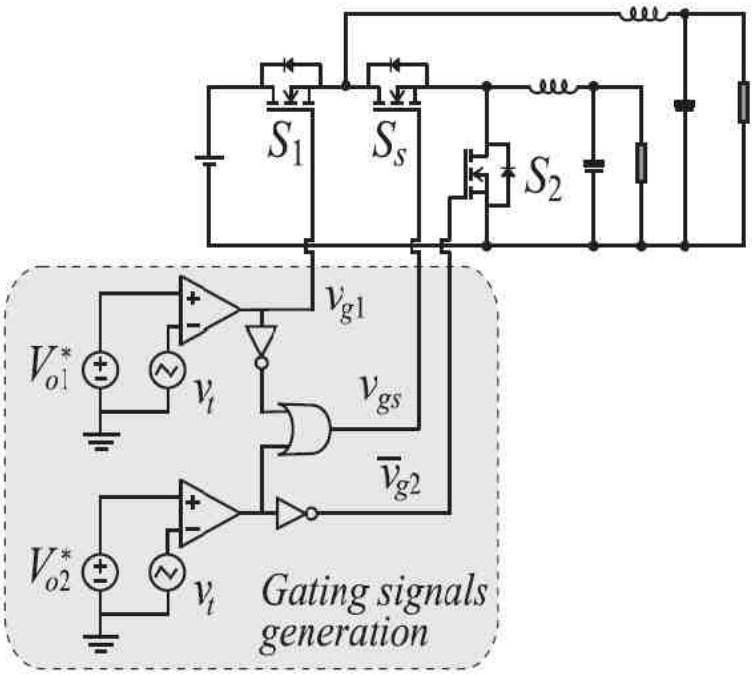

Fig. 3.6. Pulse width modulation strategy for mode 1

to this OR gate is the complement of the gating signal for switch S_1 and the direct output for the gating signal for switch S_2. As a result, the states of the three switches is never same hence avoiding a short circuit.

Control

Two proportional plus integral controllers are used in this mode. One controller is aimed at the maximum power point tracking of the PV panel. The second controller is aimed at maintaining a constant voltage across the battery. The maximum power point tracking of the PV panel is done by the Perturb & Observe Method described in Chapter 2. This is a closed loop controller.

It reads the power from the PV panel as an input. The control logic is as explained for the Perturb & Observe method. This output becomes the input for the pulse width modulation thereby generating the gating signal for switch S_1.

3.3.2 Mode 2 - Battery to DC link

This mode is as shown in Fig the PV panel is not functional. The converter works as a boost converter. The source of energy is provided by the battery that has been maintained at a specific voltage during Mode 1 operation. This mode is operational during low light conditions when the power generated from the PV panel is very low. The converter in this case works as a boost converter. Figure 3.7 shows the circuit diagram for Mode 2 operation.

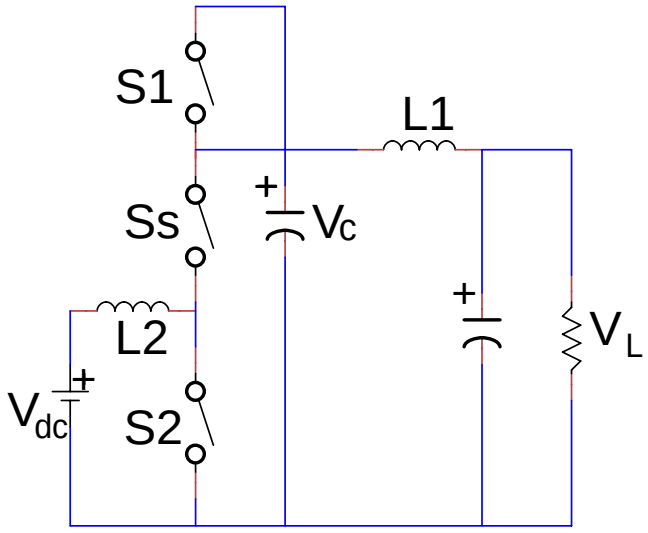

Fig. 3.7. Mode 2 Circuit Diagram

Pulse Width modulation

The Pulse Width modulation strategy is same as the one employed in mode 1. Here also, the three switches have to avoid a short circuit condition thereby all three cannot be ON at any given point of time. The control aspect varies slightly from mode 1. This is explained in the next section.

Control

In this mode, there are two closed loop controls.

- Bottom loop

  Figure 3.8 shows the control strategy for the capacitor voltage. The output of this controller is given to the gate signal of switch S_2.

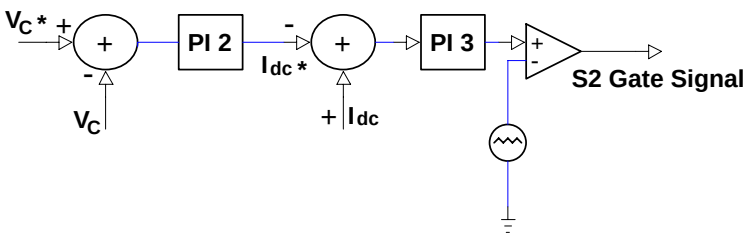

Fig. 3.8. Control loop for switch S_2

This loops aims at maintaining a constant voltage across the capacitor V_c. The control strategy is given in Fig. It comprises of two proportional plus integral controllers. The first controller compares the capacitor voltage with a set refernce voltage. The output of the first proportional plus integral controller forms the input to the second controller. This vaue is compared to the current I_{DC} coming from the battery and flowing through the inductor. The output of this controller is used for the pulse width modulation to control the duty cycle by the gating signal of the bottom switch S_2.

- Top loop

  Figure 3.9 shows the control strategy for the load voltage. The output of this controller is given to switch S_1. This loop aims at maintaining a voltage across

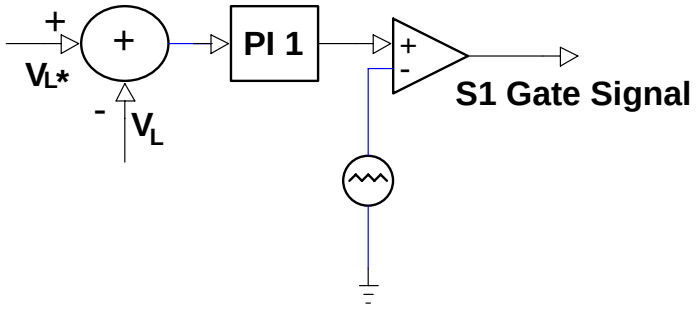

Fig. 3.9. Control loop for switch S_1

the DC link. This value is set by the user which is usually 45V for DC micro grid applications. Here there is only one proportional plus integral controller that has its input as the error signal calculated from the difference of the set reference voltage and the actual DC link voltage at the micro grid. This signal generates the pulse width modulation to control the top switch S_1.

3.3.3 Mode 3 - Grid to battery

This mode aims at charging the battery in absence of the PV panel. This condition will arise when the battery is discharged and the light exposure reduces, thereby making the PV panel non functional. The converter works as a simple buck converter.

Pulse Width Modulation

The pulse width modulation strategy used for this mode is different than the one used for modes 1 and 2. The top switch S_1 is always kept OFF. This keeps the PV

panel and the capacitor V_c disconnected from the circuit. The states of the switches S_2 and S_s is always complementary in order to avoid the situation of a short circuit.

Control

One proportional plus integral controller is used in this mode. The actual voltage across the battery is measured and compared with the set voltage at which the battery is desired to be charged. The output of this controller is then used for the pulse width modulation as discussed in the previous to modes.

4. SIMULATION AND EXPERIMENTAL RESULTS

4.1 Introduction

This chapter gives the simulated results for each mode. The circuit digram for each mode along with the detailed analysis of the simulation results is also given. Further, the hardware employed for experimental results is described. The experimental results are analyzed and compared to the simulation results and theoretical expectations in order to validate the configuration.

4.2 Simulation Results

This section deals with the simulation results for the three modes. Every mode is discussed individually. All simulations have been done using PSIM Version 9.2 .

It is important to note that for the purpose of simulation, all the components used are ideal. Also, the pulse width modulation is simulated using comparators and digital gates. The control logic is implemented with the use of a dynamic link library block. This control logic is written in C. The use of dynamic link libraries or DLLs helps promote modularization of code, code reuse, efficient memory usage, and reduced disk space. Therefore, the operating system and the programs load faster, run faster, and take less disk space on the computer [62].

The parameter values for the purpose of simulation are as follows:

- L_1 = 10mH
- L_2 = 5mH
- DC link or microgrid voltage = 45 volts
- Battery reference voltage = 24 volts

- Capacitance in parallel with the PV panel = 1000uF
- PI gains for MPPT controller : $K_p = 2$, $K_i = 200$
- PI gains for battery voltage : $K_p = 5.5$, $K_i = 20$

4.2.1 Mode 1 - PV to battery and DC link

This mode involved all three components i.e. the PV, the battery and the load at the DC link. This mode will be operational during the day time when the PV is the main source of energy. The aim of this mode is to utilize maximum energy from the PV in order to charge the battery and also to supply energy to the load at the DC link. Both these aims need to be fufilled while ensuring maximum power point tracking of the PV.

In this simulation, a triangular wave input is given to simulate varying sunlight. The aim of this is to test the control strategy for the maximum power point tracking as well as to test if the voltage across the battery is maintained at a specified voltage. Figure 4.1(a) shows the power delivered by the panel for a set of incident light and temperature parameters. This power is varied within a range of 250W with a triangular input of 1Hz. From Figure 4.1(a) (bottom) it can be verified that the maximum power output follows the maximum theoretical power output of the PV. This proves that the maximum power point tracking is achieved for the PV even with varying input conditions. Further, from Figure 4.1(b) it is seen that the voltage across the battery is maintained at a constant voltage of 24 volts. Apart from this, the voltage across the load at the DC link follows the voltage at the output of the PV. Thereby, all the goals of this mode are met. Another important point to note is the inductor current. This converter is meant to operate in continuous conduction mode as can be seen from Figure 4.1(c).

4.2.2 Mode 2 - Battery to DC link

This mode does not involve the PV. As described in Chapter 3, this mode of operation will take place when there isn't enough sunlight available and the battery will supply energy. Here, the control strategy is such that the capacitor voltage is controlled, threrby maintaining a specific voltage across the load at the DC link. From Figure 4.2 it is observed that the voltage at the DC link is maintained at a constant vaue of 45 volts. Also, the voltage across the capacitor is maintained at 50 volts as specified to the controller. This verifies Mode 2 operation.

4.2.3 Mode 3 - Grid to battery

This mode is in operation when the battery is not charged as well as the PV is not functional. The aim in this mode is to recharge the battery using the energy from the grid. From Figure 4.3 it is clear that the voltage across the battery is maintained at 24 volts. This implies that the control for this mde is working and it is verified.

4.3 Hardware

This section gives the details of the hardware that is used for the experimental set up. The specifications of every component is described along with how it has been used for getting the experimental results.

4.3.1 Photovoltaic panel

The photovoltaic panel used is a Goliath 140 Watt solar panel module. This panel has the following specifications :

- Nominal output voltage = 12 volts
- Operating voltage (V_{mp} = 17.8 volts)
- Operating current (I_{mp} = 7.87 volts)

- Open circuit voltage (V_{oc} = 21.7 volts)
- Weight = 28 pounds
- Dimensions = 59 x 28 x 3.2 inches

All these parameters are measured under standard test conditions of 1 sun. This means the light intensity is equivalent of 1 sun that amounts to 14,000 watts of lamps placed at a distance of 1 meter from the panel. Light intensity is measure in watts per square meter and power is measured in watts. For experimental purposes and due to the restrictions of space in the laboratory, lamps are used to irradiate the panel. These lamps are equivalent to a tenth of the sun's energy. They are equivalent to 1400 watts. Hence all values are a tenth of the standard test conditions that are given in the panel specifications.

4.3.2 Microcontroller

The microcontroller used to implement the control logic is the Microchip dsPIC33F J64MC802. This is a 28 pin SPDIP chip with 6 analog input pins. MPLAB IDE along with a C compiler is used for debugging and programming the chip. All the proportional plus integral controllers required in this set up are implemented using Euler's method as the digital format is used for computation of the control logic. The chip reads the appropriate voltage and current values from its analog input pins. The control logic processes these values and the output is given as the trigger signals for the three IGBTs. The internal PWM module of the chip is used. Supply to this chip is gien from the battery to avoid disruption in supply to the chip and thereby , the entire control system.

4.3.3 IGBT, IGBT Driver & Interfacing Board

The switches employed are IGBTs as shown in Figure 4.5(a). The IGBTdrivers used in this set up are the CONCEPT 2SC0108T2A0-17 (Figure 4.5(b). An interme-

diate board is utilized to interface the controller board with the IGBT driver board. This board is shown in Figure 4.5(c). The purpose of this board is to route the appropriate control signals coming from the main controller board to the correct pins of the IGBT driver board.

4.3.4 Controller Board

This board has been specially designed for this set up. It houses the microcontroller, two current sensors and the voltage regulator and other peripheral components. Analog or digital inputs can be given to the microcontroller via this board. Also, the trigger signal for the IGBTs is also given by this controller board after it processes the variables according to the logic programmed on the chip. Figure 4.7 shows the assembled board.

4.3.5 Lamps

As the experimental set up is indoors, lamps are used to substitute sunlight. In this set up four lamps are used summing up to 1400 watts. These are placed at a distance of 1 meter from the panel to simulate irradiance equivalent to the light intensity of a tenth of the sun.

4.3.6 Battery

A 12 volt rechargable battery is used. It is the AJC D18S. This battery is used to supply power to the microcontroller and the two current sensors onboard the controller board. The voltage is dropped down to a suitabe value by the use of a voltage divider.

4.3.7 Current Sensors

Two current sensors are used in this set up. One sensor is used to measure the current output of the PV panel. The second sensor is used to measure the battery current. The current sensor used is the ACS756 by Allegro Microsystems.

4.3.8 Oscilloscope

A power oscilloscope is used to measure the voltages and currents accurately. The oscilloscope used here is the DS07014B by Agilent Technologies as shown in Figure 4.9.

4.3.9 Load Resistors

Load resistors capable of high power dissipation are used. This is shown in Figure 4.10.

4.3.10 Capacitor

A capacitor bank is used to include 1000uF of capacitance in the circuit. This capacitor is connected in parallel to the PV panel.This is shown in Figure 4.11.

4.4 Experimental Results

The experimental results are taken at varying loads of 5Ω, 10Ω and 20Ω. This is done to test the Maximum Power Point Tracking logic of the controller in Mode 1. The results of with and without the Maximum Power Point Tracking are compared to show the advantage of the controller as against its absence.

The Table 4.1 shows the results with and without the MPPT for the different resistor values.

Table 4.1
Voltage, Current and Power values for the system with and without Maximum Power Point Tracking

Load Resistance (Ω)	**Parameter**	**Without MPPT**	**With MPPT**
5	Voltage (V)	3	7.5
	Current (A)	0.5	0.45
	Power (W)	1.5	**3.375**
10	Voltage (V)	5	8.5
	Current (A)	0.5	0.4
	Power (W)	2.5	**3.4**
20	Voltage (V)	8	13
	Current (A)	0.38	0.26
	Power (W)	3.04	**3.45**

From the Table 4.1, it is clear that with the MPPT controller, the power is always maintained at approximately 3.4 watts. This verifies that the MPPT controller is working with any varying load. The results given in the table are shown in Figure 4.12. The power is calculated as the product of the voltage (green) and current (yellow) values.

Another way of testing whether the MPPT controller is functional is to check the duty cycle of the trigger signal generated by the controller. For different values of load, this duty cycle changes as per the control logic, but yet maintains the maximum power output. This is shown in Figure 4.13.

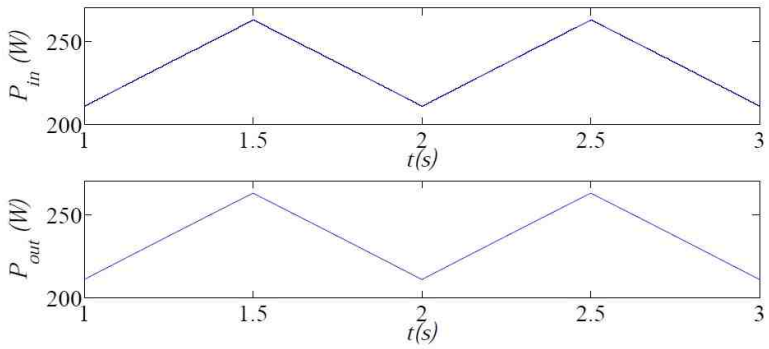

(a) Maximum Power Point Tracking

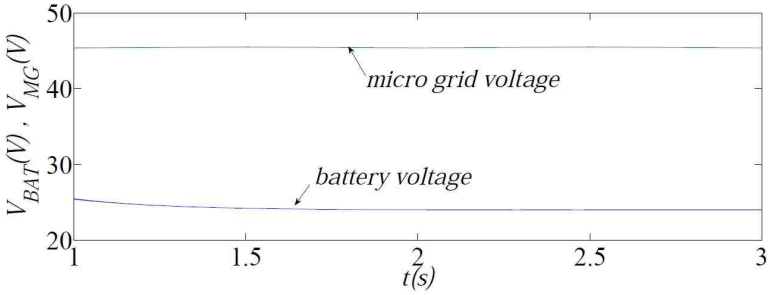

(b) Battery and DC link/microgrid voltage

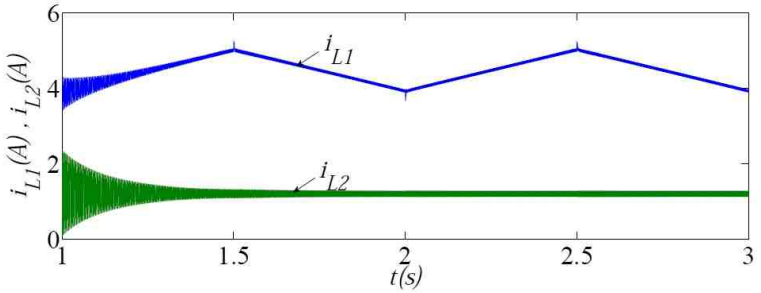

(c) Inductor Current

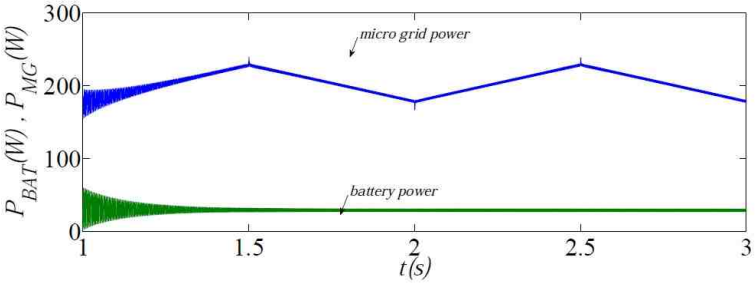

(d) Power delivered from PV panel to the microgrid and battery

Fig. 4.1. Mode 1 Simulation Results

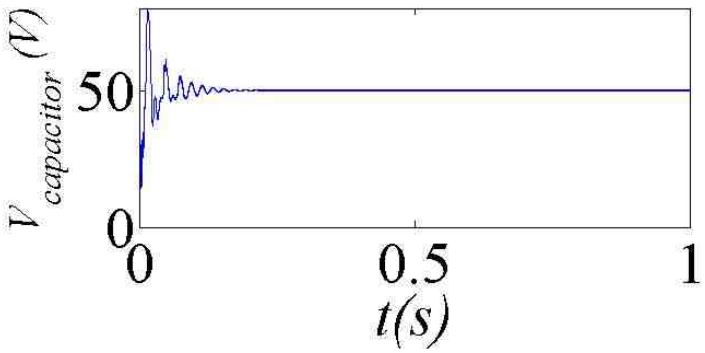

(a) Capacitor Voltage

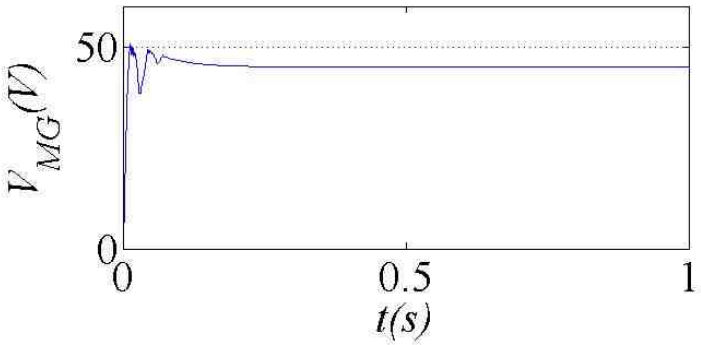

(b) DC link or microgrid voltage

Fig. 4.2. Mode 2 Simulation Results

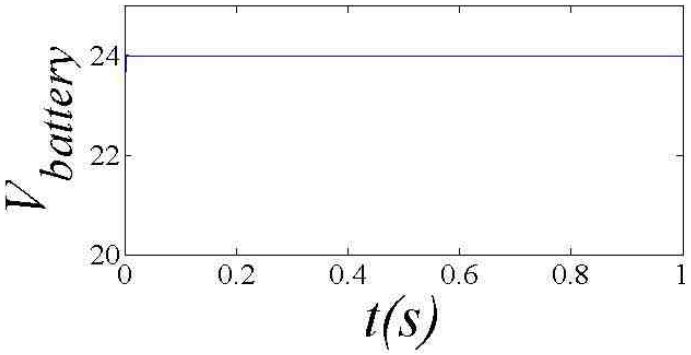

Fig. 4.3. Mode 3 Simulation Result: Voltage across the Battery

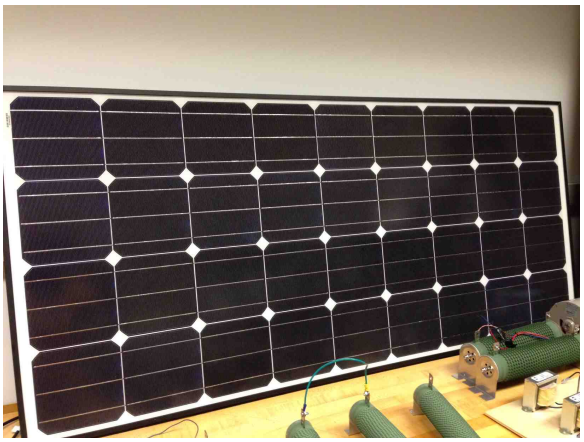

Fig. 4.4. Photovoltaic Panel

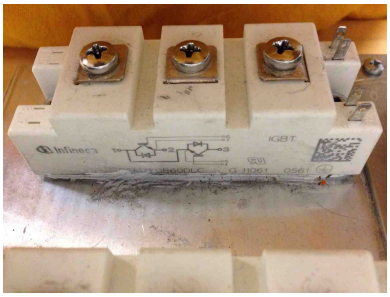

(a) IGBT

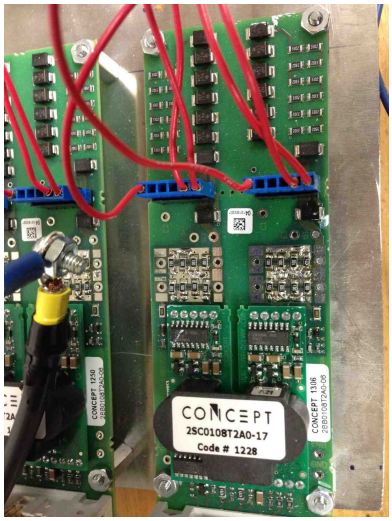

(b) IGBT Driver

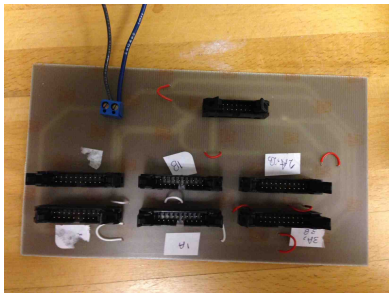

(c) Interfacing Board

Fig. 4.5. IGBT, IGBT Driver and the Interfacing Board

Fig. 4.6. Battery D18S

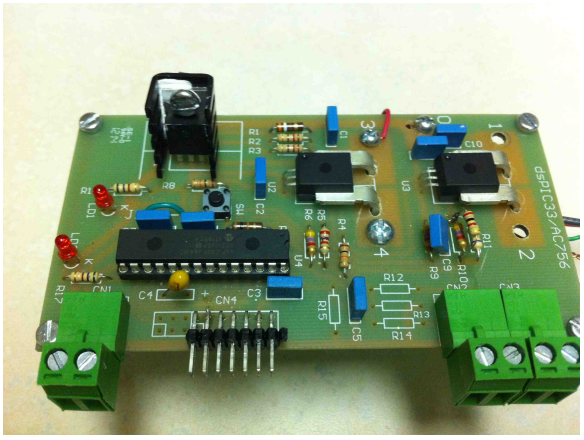

Fig. 4.7. Controller Board

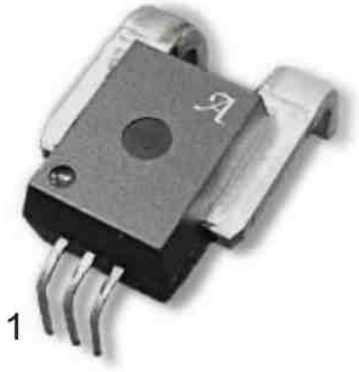

Fig. 4.8. Current Sensor ACS756

Fig. 4.9. Oscilloscope

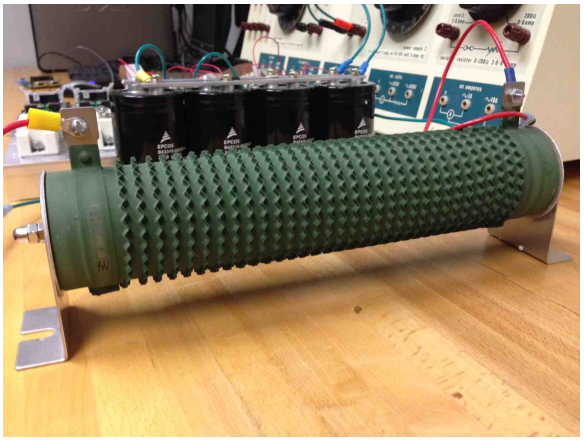

Fig. 4.10. Load Resistors

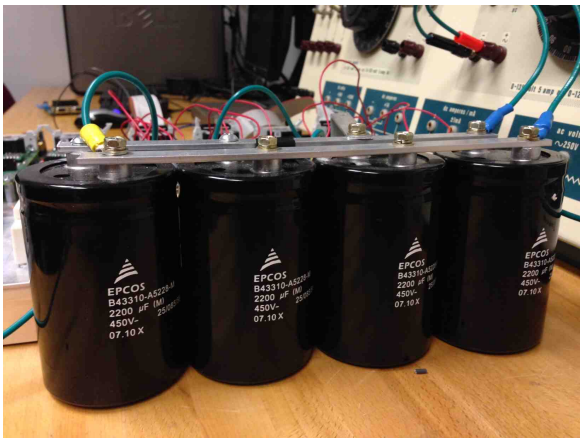

Fig. 4.11. Capacitor bank

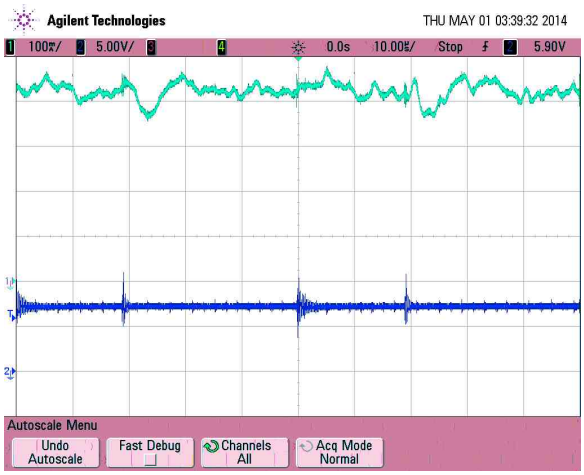

(a) 5 Ω

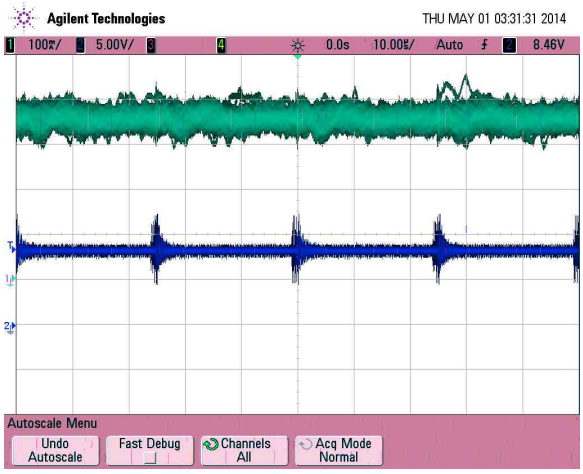

(b) 10 Ω

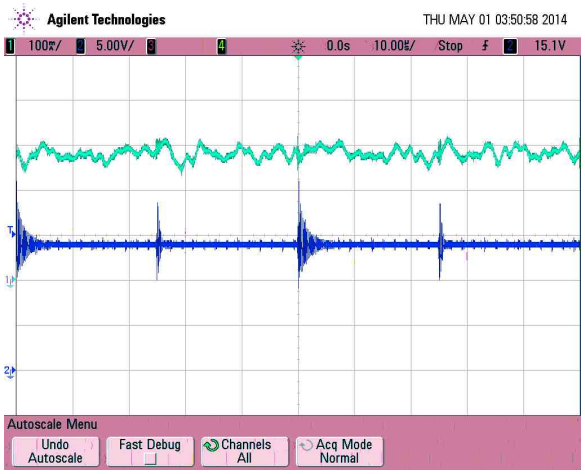

(c) 20 Ω

Fig. 4.12. Voltage (green) and Current (yellow) readings for 5Ω, 10Ω and 20Ω load.

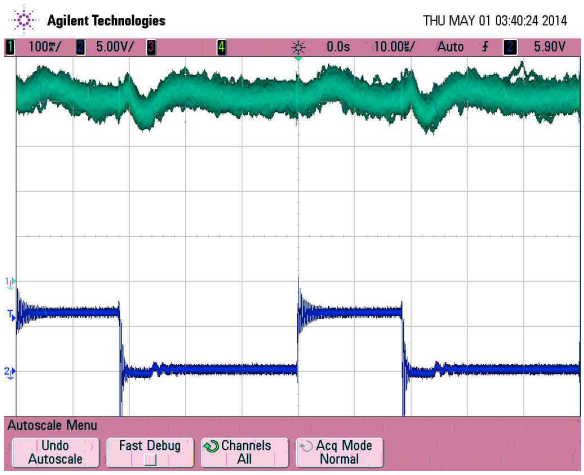

(a) 5 Ω

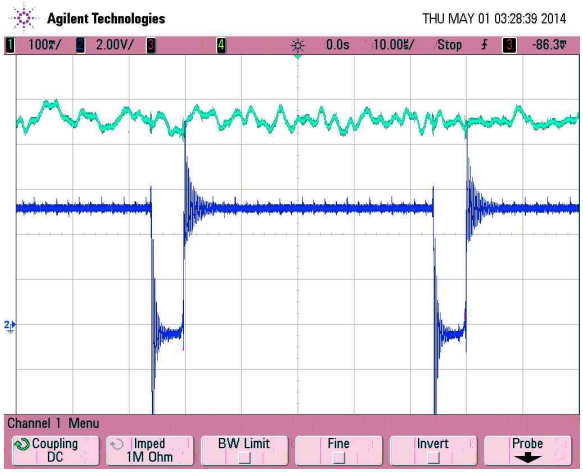

(b) 10 Ω

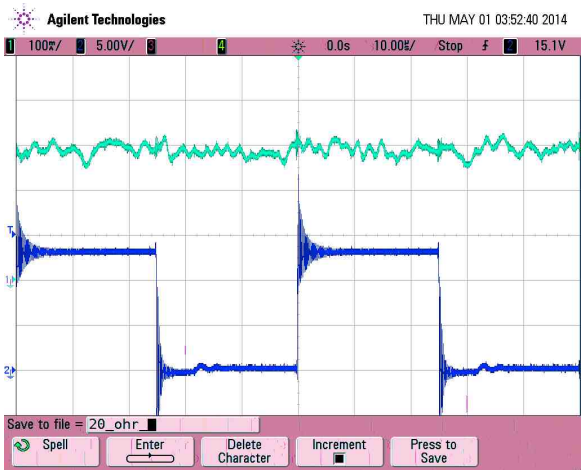

(c) 20 Ω

Fig. 4.13. Duty Cycle (green) for 5Ω, 10Ω and 20Ω load.

5. FUTURE WORK, IMPROVEMENTS AND CONCLUSION

5.1 Future Work

This model for the converter is not fully tested. From the three modes, only Mode 1 is tested for experimental results. Simulation results show that all three modes can operate to give desired results. These three modes need to be tested individually. Once this stage gives satisfactory results, all the three modes need to be combined in order to test the entire system in different irrandiance conditions. Also, various combinations of situations needs to be simulated in order to test if the system can switch between modes by itself. This makes it a smart system.

5.2 Improvements

A number of improvements can be made to the current system in order to make it more user friendly and also to make it a better prototype for testing purposes.

1. Addition of an external display to monitor variables on the microcontroller: This makes it easier to make changes to certain parameters without disconnecting the chip from the board and connecting it to a computer.

2. Addition of an external keypad: This would enable the user to change values of the PI controller gains online and see its resulting changes.

3. Addition of an amplifier on the main controller board: This is a helpful feature when the irrandiance on the panel is very low and calibration of the corresponding current levels becomes difficult.

5.3 Conclusion

Renewable energy is growing and gradually, solar power has been entering the residential market. As stated in [63], since the 1970s, when the first PV system for a residence was installed, there have been 150,000 PV installations as per industry experts. Also, federal and state rebates help promote the use of solar power. An average American hosuehold uses 10,000kilowatts of electricityper year. Residential photovoltaic systems are groups together to form an array and create about 3kWh to 10kWh systems. A 5kWh system generates an average of 6,000 kilowatts per year. With a system as describe in this thesis, the excess energy generated can have the utility company credit the user if excess energy is generated. More efficient solar panels are being developed in order to capture maximum energy from the sun. Despite all these benefits, cos remains the single barrier for homeowners.

6. SUMMARY

The aim of this thesis is:

- To replace the constant DC source with a photovoltaic panel.
- To implement maximum power point tracking of the photovoltaic panel.
- To simulate the various modes of operation for this configuration under different irradiance and power demanding situations.
- To design a general purpose board in order to test all the three modes experimentally.

All of these goals have been met and the results are shown and analyzed.

LIST OF REFERENCES

LIST OF REFERENCES

[1] F. A. Brooks, "Solar energy and its use for heating water in california," *Sunworld*, vol. 12, no. 3, pp. 88–92, 1988.

[2] N. S. Lewis, "Toward cost-effective solar energy use," *science*, vol. 315, no. 5813, pp. 798–801, 2007.

[3] M. Calais, J. Myrzik, T. Spooner, and V. G. Agelidis, "Inverters for single-phase grid connected photovoltaic systems-an overview," in *Power Electronics Specialists Conference, 2002. pesc 02. 2002 IEEE 33rd Annual*, vol. 4, pp. 1995–2000, IEEE, 2002.

[4] http://solarenergy.com/, "Solar energy-the latest news, technology and events," 2013. Last accessed: May 2014.

[5] M. Bellis, "Definition of a solar cell-history of solar cells. http://inventors.com," Last accessed: June 2014.

[6] T. Tiedje, G.Yablonovitch, G. Cody, and B. Brooks, "Limiting efficiency of silicon solar cells," *Electron Devices, Electronics, IEEE Transactions*, vol. ED-31, May 1984.

[7] A. Slaoui and R. Collins, "Inorganic photovoltaic solar cells: Silicon and beyond," *MRS Bull*, March 2007.

[8] M. Grätzel, "Photoelectrochemical cells," *Nature*, vol. 414, no. 6861, pp. 338–344, 2001.

[9] F. Blaabjerg, R. Teodorescu, M. Liserre, and A. V. Timbus, "Overview of control and grid synchronization for distributed power generation systems," *Industrial Electronics, IEEE Transactions*, vol. 53, no. 5, pp. 1398–1409, 2006.

[10] T. Markvart, *Solar electricity*. John Wiley & Sons, 2000.

[11] F. Yang, M. Shtein, and S. R. Forrest, "Controlled growth of a molecular bulk heterojunction photovoltaic cell," *Nature Materials*, vol. 4, no. 1, pp. 37–41, 2004.

[12] M. A. Green, "Third generation photovoltaics: solar cells for 2020 and beyond," *Physica E: Low-dimensional Systems and Nanostructures*, vol. 14, no. 1, pp. 65–70, 2002.

[13] A. Gonzalez, F. Echavarren, and R. Gomez, "A sensitivities computation method for reconfiguration of radial networks," *Power Systems, Electronics, IEEE Transactions*, vol. 27, August 2012.

[14] P. P. Barker and R. W. de Mello, "Determining the impact of distributed generation on power systems. i. radial distribution systems," in *Power Engineering Society Summer Meeting, 2000. IEEE*, vol. 3, pp. 1645–1656, IEEE, 2000.

[15] V. Mehta and R. Mehta, *Distribution Systems- General, Principles of Power System: Including Generation, Transmission, Distribution, Switchgear and Protection: for BE/B.Tech, AMIE and Other Engineering Examinations*. S.Chand Publications, 2005.

[16] F. Zhang and C. S. Cheng, "A modified newton method for radial distribution system power flow analysis," *Power Systems, IEEE Transactions*, vol. 12, no. 1, pp. 389–397, 1997.

[17] M. T. Doyle, "Reviewing the impacts of distributed generation on distribution system protection," in *Power Engineering Society Summer Meeting, 2002 IEEE*, vol. 1, pp. 103–105, IEEE, 2002.

[18] D. Boroyevich, I. Cvetkovic, D. Dong, R. Burgos, F. Wang, and F. Lee, "Future electronic power distribution systems - a contemplative view," *Optimization of Electrical and Electronic Equipment(OPTIM)*, May 2010.

[19] B. Zhao, Q. Yu, and W. Sun, "Extended phase shift control of isolated bidirectional dc-dc converter for power distribution in microgrid," *Power Electronics, IEEE Transactions*, vol. 27, November 2012.

[20] T. Gonen, *Electric power distribution engineering*. CRC press, 2014.

[21] F. Blaabjerg, Z. Chen, and S. Kjaer, "Power electronics as efficient interface in dispersed power generation systems," *Power Electronics, IEEE Transactions*, vol. 19, September 2004.

[22] "D.pl09-4-000," *Smart Grid Policy U.S. Federal Energy Regulatory Comission(FERC)*, 2009.

[23] A. Communications, "Power electronics: The hidden technology that makes the modern world run," May 2013. http://www.abb.com/cawp/seitp202/85b14cadbc1d544bc1257b5b003de5af.aspx.

[24] E. Koutroulis, K. Kalaitzakis, and N. C. Voulgaris, "Development of a microcontroller-based, photovoltaic maximum power point tracking control system," *Power Electronics, IEEE Transactions*, vol. 16, no. 1, pp. 46–54, 2001.

[25] S. B. Kjaer, J. K. Pedersen, and F. Blaabjerg, "A review of single-phase grid-connected inverters for photovoltaic modules," *Industry Applications, IEEE Transactions*, vol. 41, no. 5, pp. 1292–1306, 2005.

[26] D.Ghodke, K.Chatterjee, and B.Fernandes, "Modified soft-switched three-phase three level dc dc converter for high-power applicaitons having extended duty cycle range," *IEEE Transactions Industrial Electronics*, vol. 59, pp. 3362–3372, September 2013.

[27] M. Pahlevaninezhad, J. Drobnik, P. Jain, and A. Bakhshai, "A load adaptive control approach for a zero-voltage-switching dc/dc converter used for electric vehicles," *Industrial Electronics, IEEE Transactions*, vol. 59, pp. 920–933, February 2012.

[28] M. Shen, F. Z. Peng, and L. M. Tolbert, "Multilevel dc-dc power conversion system with multiple dc sources," *Power Electronics, IEEE Transactions*, vol. 23, no. 1, pp. 420–426, 2008.

[29] L. Ni, D. Patterson, and J. Hudgins, "High power current sensorless bidirectional 16-phase interleaved dc-dc converter for hybrid vehicle application," *Power Electronics, IEEE Transactions*, vol. 27, pp. 1141–1151, March 2012.

[30] E. dos Santos, "Dual-output dc-dc buck converters with bidirectional and unidirectional characteristics," *Power Electronics, IET*, vol. 6, pp. 999–1009, May 2013.

[31] M. Belloni, E. Bonizzoni, and F. Maloberti, "On the design of single-inductor double-output dc-dc buck, boost and buck-boost converters," in *Electronics, Circuits and Systems, 2008. ICECS 2008. 15th IEEE International Conference*, pp. 626–629, August 2008.

[32] Rojas-Gonzalez, M.A., Torres, J., E. Sanchez-Sinencio, and P. Kumar, "An integrated dual-output buck converter based on sliding mode control," in *Circuits and Systems (LASCAS), 2012 IEEE Third Latin American Symposium*, pp. 1–4, February 2012.

[33] K. Ogata and Y. Yang, "Modern control engineering," 1970.

[34] R. C. Dorf, *Modern control systems*. Addison-Wesley Longman Publishing Co., Inc., 1995.

[35] N. Aziz, M. Hussain, and I. Mujtaba, "Performance of different types of controllers in tracking optimal temperature profiles in batch reactors," *Computers & Chemical Engineering*, vol. 24, no. 2, pp. 1069–1075, 2000.

[36] F. G. Shinskey, *Feedback controllers for the process industries*. McGraw-Hill Professional, 1994.

[37] D. G. Luenberger and Y. Ye, *Linear and nonlinear programming*, vol. 116. Springer, 2008.

[38] D. A. Lawrence and W. J. Rugh, "Gain scheduling dynamic linear controllers for a nonlinear plant," *Automatica*, vol. 31, no. 3, pp. 381–390, 1995.

[39] G. Escobar, R. Ortega, H. Sira-Ramirez, J. Vilain, and I. Zein, "An experimental comparison of several nonlinear controllers for power converters," *Control Systems, IEEE*, vol. 19, no. 1, pp. 66–82, 1999.

[40] B. Lantos and L. Marton, *Nonlinear Control of Vehicles and Robots*. Springer, 2011.

[41] O. Wasynezuk, "Dynamic behavior of a class of photovoltaic power systems," *Power Apparatus and Systems, IEEE Transactions*, no. 9, pp. 3031–3037, 1983.

[42] Z. Yan, L. Fei, Y. Jinjun, and D. Shanxu, "Study on realizing mppt by improved incremental conductance method with variable step-size," in *Industrial Electronics and Applications, 2008. ICIEA 2008. 3rd IEEE Conference*, pp. 547–550, IEEE, 2008.

[43] T. Esram and P. L. Chapman, "Comparison of photovoltaic array maximum power point tracking techniques," *IEEE TRANSACTIONS ON ENERGY CONVERSION EC*, vol. 22, no. 2, p. 439, 2007.

[44] A. K. Abdelsalam, A. M. Massoud, S. Ahmed, and P. Enjeti, "High-performance adaptive perturb and observe mppt technique for photovoltaic-based microgrids," *Power Electronics, IEEE Transactions*, vol. 26, no. 4, pp. 1010–1021, 2011.

[45] M. A. Masoum, H. Dehbonei, and E. F. Fuchs, "Theoretical and experimental analyses of photovoltaic systems with voltageand current-based maximum power-point tracking," *Energy conversion, IEEE transactions*, vol. 17, no. 4, pp. 514–522, 2002.

[46] D. C. anf PCM, R. Pontes, D. Oliveira Jr, D. Riffel, R. de Oliveira, and S. Mesquita, "Control method of a photovoltaic powered reverse osmosis plant without batteries based on maximum power point tracking," in *Transmission and Distribution Conference and Exposition: Latin America, 2004 IEEE/PES*, pp. 137–142, IEEE, 2004.

[47] T. Noguchi, S. Togashi, and R. Nakamoto, "Short-current pulse-based maximum-power-point tracking method for multiple photovoltaic-and-converter module system," *Industrial Electronics, IEEE Transactions*, vol. 49, no. 1, pp. 217–223, 2002.

[48] T. Noguchi, S. Togashi, and R. Nakamoto, "Short-current pulse-based maximum-power-point tracking method for multiple photovoltaic-and-converter module system," *Industrial Electronics, IEEE Transactions*, vol. 49, no. 1, pp. 217–223, 2002.

[49] N. Femia, D. Granozio, G. Petrone, G. Spagnuolo, and M. Vitelli, "Optimized one-cycle control in photovoltaic grid connected applications," *Aerospace and Electronic Systems, IEEE Transactions*, vol. 42, no. 3, pp. 954–972, 2006.

[50] B. Liu, S. Duan, F. Liu, and P. Xu, "Analysis and improvement of maximum power point tracking algorithm based on incremental conductance method for photovoltaic array," in *Power Electronics and Drive Systems, 2007. PEDS'07. 7th International Conference*, pp. 637–641, IEEE, 2007.

[51] N. Femia, G. Petrone, G. Spagnuolo, and M. Vitelli, "Optimization of perturb and observe maximum power point tracking method," *Power Electronics, IEEE Transactions*, vol. 20, no. 4, pp. 963–973, 2005.

[52] N. Fermia, D. Granozio, G. Petrone, and M. Vitelli, "Predictive & adaptive mppt perturb and observe method," *Aerospace and Electronic Systems, IEEE Transactions*, vol. 43, no. 3, pp. 934–950, 2007.

[53] T. Tafticht, K. Agbossou, M. Doumbia, and A. Chériti, "An improved maximum power point tracking method for photovoltaic systems," *Renewable Energy*, vol. 33, no. 7, pp. 1508–1516, 2008.

[54] D. Hohm and M. Ropp, "Comparative study of maximum power point tracking algorithms using an experimental, programmable, maximum power point tracking test bed," in *Photovoltaic Specialists Conference, 2000. Conference Record of the Twenty-Eighth IEEE*, pp. 1699–1702, IEEE, 2000.

[55] T. Esram, Chapman, and P. L, "Comparison of photovoltaic array maximum power point tracking techniques," *IEEE TRANSACTIONS ON ENERGY CONVERSION EC*, vol. 22, no. 2, p. 439, 2007.

[56] K. Hussein, I. Muta, T. Hoshino, and M. Osakada, "Maximum photovoltaic power tracking: An algorithm for rapidly changing atmospheric conditions," *IEEE Proceedings-Generation, Transmission and Distribution*, vol. 142, no. 1, pp. 59–64, 1995.

[57] G. K. Ottman, H. F. Hofmann, A. C. Bhatt, and G. A. Lesieutre, "Adaptive piezoelectric energy harvesting circuit for wireless remote power supply," *Power Electronics, IEEE Transactions*, vol. 17, no. 5, pp. 669–676, 2002.

[58] P. Bhatnagar and R. Nema, "Maximum power point tracking control techniques: State-of-the-art in photovoltaic applications," *Renewable and Sustainable Energy Reviews*, vol. 23, pp. 224–241, 2013.

[59] S. Jain and V. Agarwal, "Comparison of the performance of maximum power point tracking schemes applied to single-stage grid-connected photovoltaic systems," *IET Electric Power Applications*, vol. 1, no. 5, pp. 753–762, 2007.

[60] K. S. Lee, "Maximum power point tracking method," January 2011. Last accessed 20 May 2014. US Patent App. 13/522,697.

[61] H. Patel and V. Agarwal, "Maximum power point tracking scheme for pv systems operating under partially shaded conditions," *Industrial Electronics, IEEE Transactions*, vol. 55, no. 4, pp. 1689–1698, 2008.

[62] A. I. 815065, "What is a dll? http://support.microsoft.com/kb/815065," Last accessed: June 2014.

[63] J. Connors, "The evolution of solar power. www.hgtvremodels.com/home-systems/the-evolution-of-solar-power/index.html," Last accessed: June 2014.